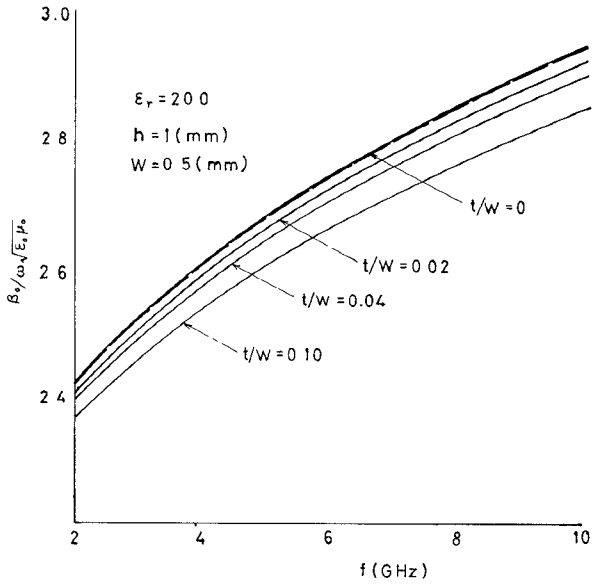

Fig. 2. Relative phase constant ($\beta_0/\omega\sqrt{\epsilon_0\mu_0}$). Solid line represents present method and broken line represents Cohn's results.

(12) is satisfied only at the center of the slot instead of over the slot range [4]. In this short paper we obtain the solution by applying the following numerical calculation method. We multiply the first equation of (12) by $m_{1y}(x)$ and the second equation by $m_{2y}(x)$, and integrate in the x region using (13). On eliminating m_{10} and m_{20}, we finally obtain the following determinantal equation:

$$\{G_1(\beta_0) - G_4(\beta_0)\}\{G_2(\beta_0) - G_4(\beta_0)\} = \{G_3(\beta_0)\}^2 \tag{14}$$

where

$$G_1(\beta_0) = \int_0^\infty \frac{1}{K'^2}\left\{\frac{\omega\epsilon_0}{\kappa_0'}\alpha^2 - \frac{\kappa_0'}{\omega\mu_0}\beta_0^2\right\}J_0^2\left(\frac{W}{2}\alpha\right)d\alpha$$

$$G_2(\beta_0) = \int_0^\infty \frac{1}{K'^2}\left\{\frac{\omega\epsilon_0}{\kappa_0'}\cdot\frac{1+(\epsilon_r\kappa_0'/\kappa')\tan(\kappa' h)}{1-(\kappa'/\epsilon_r\kappa_0')\tan(\kappa' h)}\alpha^2 - \frac{\kappa_0'}{\omega\mu_0}\cdot\frac{1-(\kappa'/\kappa_0')\tan(\kappa' h)}{1+(\kappa_0'/\kappa')\tan(\kappa' h)}\beta_0^2\right\}J_0^2\left(\frac{W}{2}\alpha\right)d\alpha$$

$$G_3(\beta_0) = \frac{\pi}{W}\frac{\gamma_0'}{\omega\mu_0}\operatorname{csch}(\gamma_0' t) - \frac{2\pi}{W}\sum_{n=1}^{\infty}\frac{1}{K_n'^2}\left\{\frac{\omega\epsilon_0}{\gamma_n'}\alpha_n^2 - \frac{\gamma_n'}{\omega\mu_0}\beta_0^2\right\}\cdot\operatorname{csch}(\gamma_n' t)J_0^2\left(\frac{W}{2}\alpha_n\right)$$

$$G_4(\beta_0) = \frac{\pi}{W}\frac{\gamma_0'}{\omega\mu_0}\coth(\gamma_0' t) - \frac{2\pi}{W}\sum_{n=1}^{\infty}\frac{1}{K_n'^2}\left\{\frac{\omega\epsilon_0}{\gamma_n'}\alpha_n^2 - \frac{\gamma_n'}{\omega\mu_0}\beta_0^2\right\}\cdot\coth(\gamma_n' t)J_0^2\left(\frac{W}{2}\alpha_n\right)$$

$J_0(x)$ zero-order Bessel function.

From (14) we can find the phase constant for the lowest hybrid mode, which is expected to be in the range $\beta_0 \geq \omega\sqrt{\epsilon_0\mu_0}$. G_3 and G_4 converge very rapidly; however, the rate of convergence of G_1 and G_2 is slow but can be improved by the following procedure. When $\alpha \to \infty$, the integrand of G_1 becomes

$$F_{1\infty} = \lim_{\alpha\to\infty} F_1 = \left(\omega\epsilon_0 - \frac{\beta_0^2}{\omega\mu_0}\right)\frac{\alpha}{\alpha^2+\beta_0^2}J_0^2\left(\frac{W}{2}\alpha\right). \tag{15}$$

G_1 may be rewritten as follows:

$$G_1 = \int_0^\infty (F_1 - F_{1\infty})\,d\alpha + \int_0^\infty F_{1\infty}\,d\alpha. \tag{16}$$

The first integral on the right converges rapidly compared to G_1, while the second may be expressed in closed form

$$\int_0^\infty F_{1\infty}\,d\alpha = \left(\omega\epsilon_0 - \frac{\beta_0^2}{\omega\mu_0}\right)I_0\left(\frac{W}{2}\beta_0\right)K_0\left(\frac{W}{2}\beta_0\right) \tag{17}$$

$I_0(x)$ modified Bessel function of the first kind;
$K_0(x)$ modified Bessel function of the second kind.

Similarly for G_2

$$G_2 = \int_0^\infty (F_2 - F_{2\infty})\,d\alpha + \left(\omega\epsilon_0\epsilon_r - \frac{\beta_0^2}{\omega\mu_0}\right)I_0\left(\frac{W}{2}\beta_0\right)K_0\left(\frac{W}{2}\beta_0\right). \tag{18}$$

The computed results are shown in Fig. 2 and compared with Cohn's theory [1]. The results, supposing the thickness equal to zero, are in good agreement with Cohn's results. When the t/W ratio is 0.02, the change in the phase constant is about 1 percent, and so the effect of metal-coating thickness usually can be neglected. These numerical calculations were carried out by the electronic computer FACOM 230-60. The calculation time is about 30 s per one structure.

References

[1] S. B. Cohn, "Slot line on a dielectric substrate," *IEEE Trans. Microwave Theory Tech.*, vol. MTT-17, pp. 768–778, Oct. 1969.
[2] T. Itoh and R. Mittra, "Dispersion characteristic of slot lines," *Electron. Lett.*, vol. 7, pp. 364–365, July 1971.
[3] T. Matsumoto and M. Suzuki, "Electromagnetic fields in waveguides containing anisotropic media with time-varying parameters," *J. Inst. Electron. Commun. Eng. Jap.*, vol. 45, pp. 1680–1688, Dec. 1962.
[4] E. J. Denlinger, "A frequency dependent solution for microstrip transmission lines," *IEEE Trans. Microwave Theory Tech.*, vol. MTT-19, pp. 30–39, Jan. 1971.

Some General Observations on the Tuning Characteristics of "Electromechanically" Tuned Gunn Oscillators

J. S. JOSHI AND J. A. F. CORNICK

***Abstract*—The nature of mechanical and electronic (varactor) tuning characteristics of "electromechanically" tuned Gunn oscillators in waveguide and coaxial configurations has been investigated and their interactions studied. Some general conclusions about the family of electromechanically tuned Gunn oscillators have been drawn and their limitations pointed out. It is suggested that these limitations are imposed by a distributed circuit on a point source.**

Introduction

Gunn-effect oscillators are finding increasing applications as sources of microwave power. Their tunability and ease of operation has contributed to their popularity. Mechanically tuned Gunn oscillators in both coaxial and waveguide cavities have been reported in the literature [1]–[5]. The efforts were mainly devoted to a proper understanding of the tuning characteristics, explaining the mode switching observed in various cases, and the load dependence of Gunn-device performance. Electronic (varactor) tuning of Gunn oscillators has also been studied by many authors in both coaxial and waveguide configurations [6]–[8].

However, a majority of Gunn oscillators required for practical applications are of the "electromechanically" tuned type, and most operational modes demand high-speed electronic tuning about the frequency set by the mechanical tuning. Because of their high speed of operation, varactor diodes are invariably used for these applications. There is a lack of reported work in the literature on electromechanically tuned Gunn oscillators. Although intensive investigations have been made both on mechanical and electronic tuning of Gunn oscillators, the interaction between the two has been studied in a rather piecemeal way. The general approach taken by most workers is to optimize the performance in a restricted (mechanical) frequency range [9]. Such an approach fails to demonstrate the difficulties encountered when trying to broad-band these oscillators.

An attempt has been made here to present the tuning characteristics of electromechanically tuned Gunn oscillators in a wider perspective. In the broad frequency range in which an understanding of the tuning characteristics of electromechanically tuned Gunn oscillators is being sought, an equivalent circuit representation of the oscillator is very difficult to obtain because of the complexity of the microwave circuit involved, most elements of which are frequency

Manuscript received January 8, 1973; revised May 14, 1973.
The authors are with Mullard (Hazel Grove) Ltd., Bramhall Moor Lane, Stockport, Cheshire, United Kingdom.

dependent. A major disadvantage of an equivalent circuit representation is that it applies to one particular configuration only, and thus suffers from a loss of generality. An alternative approach has been adopted here. It involved a systematic experimental study aimed at isolating the influences of the devices (both Gunn and varactor) and the parameters of the mounting configurations on the tuning characteristics of such oscillators. On this basis, some significant conclusions regarding the mechanical and electronic tuning characteristics and their interaction are drawn.

Nature of Tuning

Gunn oscillators can generally be tuned over a wide frequency range by changing the reactance of the microwave circuit loading the device. The frequency of oscillation is determined by the requirement that the susceptance of the device be resonated by the circuit susceptance.

When a Gunn device mounted in a microwave circuit is mechanically tuned by varying the sliding short-circuit position, the frequency of oscillation corresponds to a half-wavelength (or a multiple) of the cavity length. The deviation from this behavior can be attributed to the device mounting configuration in the particular circuit, its package, and its finite capacitance. It should also be noted that as the tuning characteristic follows the half-wavelength behavior, the loaded Q of the cavity increases. Qualitative assessment of the varactor tuning has been made by various authors. On the basis of a rather simplified model, it can be deduced that the range of varactor tuning is proportional directly to the RF power coupled to the varactor, and inversely to the loaded Q of the cavity. Electronic tuning is considered to be positive if the frequency of oscillation increases as the varactor-diode reverse-bias voltage is increased (or its capacitance reduced).

Experimental Observations

Mullard CXY 19 X-band Gunn devices were used in all experiments. These are encapsulated devices in the standard S4 package with such typical parameters as: threshold voltage $V_T = 4.75$ V, threshold current $I_T = 600$ mA, operating voltage $V_G = 12.0$ V, operating current $I_G = 450$ mA, and output power $P_O = 150$ mW in a standard test cavity. Silicon tuning varactors in standard S4 package were used for electronic tuning purposes.

Waveguide System

Post-coupled waveguide-mounted Gunn oscillator configurations shown in Fig. 1 were used. The post structure plane containing both device post axes was normal to the axis of the waveguide [Fig. 1(b)]. Of the various systems available, this particular one was selected for its simplicity, ease of operation, and flexibility. It should, however, be emphasized that the choice of this configuration in no way affects the aim of establishing a broad picture of the tuning characteristics of electromechanically tuned Gunn oscillators in waveguide cavities.

A systematic experimental study of both mechanically and electromechanically tuned Gunn oscillators was conducted to investigate (where appropriate) the effects of the following: 1) Gunn and varactor device post geometry variation (post height, diameter, and axis location), 2) variation of the separation between the post axes, and 3) different varactor and Gunn devices, on the mechanical and electronic tuning characteristics. (Here the frequency at zero varactor bias as a function of sliding short-circuit position is termed the mechanical tuning characteristic of an electromechanically tuned oscillator.) The results of this study are contained in [10] and helped in establishing a broad picture of the tuning characteristics of such oscillators.

Fig. 2 contains a typical tuning characteristic of the mechanically tuned oscillator of Fig. 1(a). Fig. 3(a) and (b) shows, respectively, a typical set of mechanical and electronic tuning characteristics, while Fig. 3(c) and (d) shows, respectively, the loaded Q (at zero varactor bias) and the rectified voltage across the varactor diode as functions of the short-circuit position (the parameters of the varactor diode were $C_{T0} = 1.85$ pF, $V_{BR} = 50$ V, V_F at 1 mA $= 0.76$ V, and $C_{j6} = 0.6$ pF). It should be stressed that different parameter changes only alter the details of the above figures while the general nature of variation is maintained [10].

The following general observations on the tuning characteristics can be made.

1) The mechanical tuning characteristic [Fig. 3 (a)] maintains the half-wavelength behavior. The introduction of the varactor tuning arrangement has caused minor changes for smaller values of the

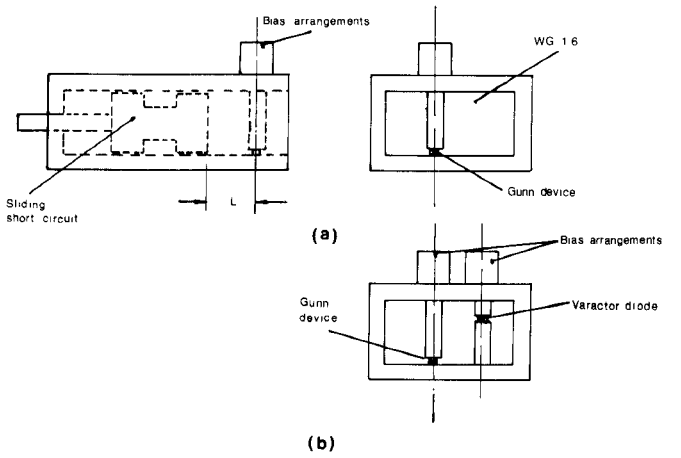

Fig. 1. Waveguide post mounting configuration for (a) mechanically tuned and (b) electromechanically tuned Gunn oscillator.

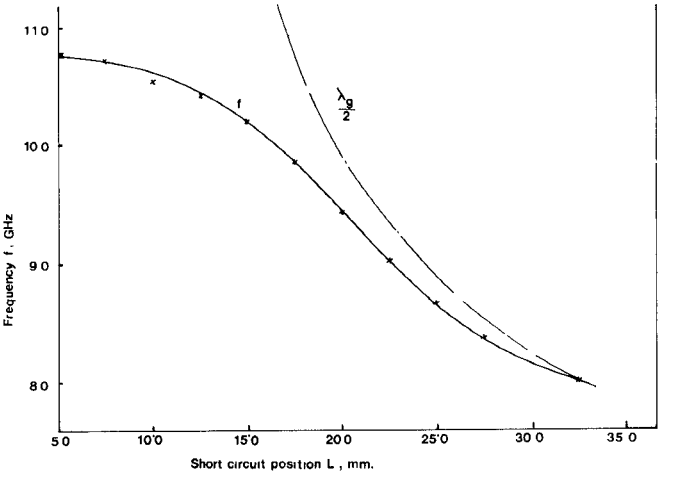

Fig. 2. Mechanical tuning characteristic of the configuration shown in Fig. 1(a). Gunn device CXY 19/31 $V_G = 13.0$ V.

short-circuit position. The additional phase shift introduced by the varactor mounting arrangement has moved the tuning characteristic to the right of the half-wavelength curve. [Compare Figs. 2 and 3 (a).]

2) The loaded Q of the cavity was measured by frequency-pulling experiments. From Fig. 3(c) it can be seen that as the mechanical tuning characteristic follows the half-wavelength behavior, the loaded Q of the cavity increases. Fig. 3(d) depicts the rectified voltage across the varactor diode as a function of the short-circuit position.

3) Fig. 3(b) shows the electronic tuning characteristic in which its decreasing nature, due to increasing loaded Q values for larger values of short-circuit position, can be clearly seen. For smaller values of the short-circuit position, although the loaded Q values are low, reduced electronic tuning range is obtained due to weak coupling to the varactor [Fig. 3(d)]. This explains the observed nature of the electronic tuning characteristic.

Coaxial System

The experiments were conducted in a 50-Ω characteristic impedance coaxial system. The configurations under investigation are shown in Fig. 4. Of the various existing forms of varactor coupling arrangements for coaxial cavity oscillators, a simple loop arrangement was adopted here. Again, the choice of this configuration in no way affects the aim of establishing a broad picture of the tuning characteristics of electromechanically tuned oscillators in coaxial cavities.

A systematic experimental study was conducted to investigate (where appropriate) the effects of the following: 1) different Gunn and varactor devices, 2) different output coupling, and 3) different varactor loop orientations on the mechanical and electronic tuning

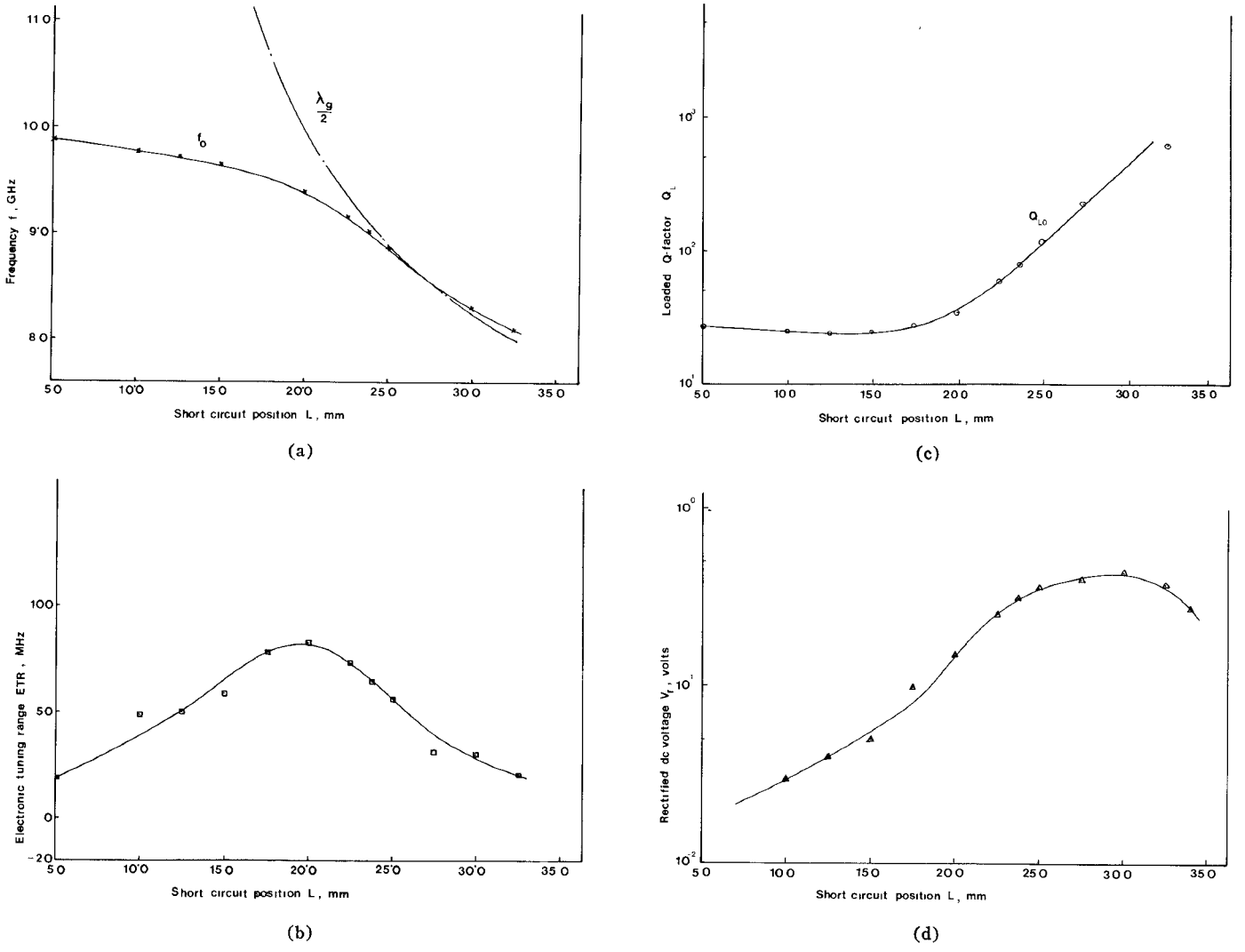

Fig. 3. (a) Mechanical tuning characteristic of the configuration shown in Fig. 1(b). Gunn device CXY 19/31 $V_G=13.0$ V. (b) Electronic tuning characteristic of the configuration shown in Fig. 1(b). Varactor tuning voltage 0–30 V. (c) Loaded Q factor (at zero varactor bias Q_{L0}) versus short-circuit position for the configuration of Fig. 1(b). (d) Varactor rectified voltage versus short-circuit position for the configuration of Fig. 1(b).

characteristics of these oscillators. The results of this experimental study are contained in [11] and helped in establishing a broad picture of the tuning characteristics of such oscillators.

Fig. 5 shows a typical tuning characteristic of the mechanically tuned oscillator of Fig. 4(a). Fig. 6 (a) and (b) shows, respectively, a typical set of mechanical and electronic tuning characteristics, while Fig. 6(c) shows the loaded Q (at zero varactor bias) as a function of the short-circuit position [11]. (The parameters of the varactor diode were $C_{T0}=2.82$ pF, $V_{BR}=40.0$ V, V_F at 1 mA $=0.93$ V, and $C_{j6}=1.52$ pF.) It should again be emphasized that different parameter changes only alter the details of Fig. 6(a), (b), and (c), while the general nature of the variation is maintained.

The following general observations on the tuning characteristics can be made.

1) The mechanical tuning characteristic Fig. 6(a) maintains the half-wavelength behavior. Only marginal changes are caused by the introduction of the varactor tuning arrangement. [Compare Figs. 5 and 6(a).]

2) The loaded Q of the cavity was measured by injection locking experiments. Fig. 6(c) indicates that as the mechanical tuning characteristic follows the half-wavelength behavior, the loaded Q of the cavity increases. The varactor-diode coupling was weak, and the measured rectified voltage across the varactor was only of the order of few tens of microvolts.

3) The electronic tuning characteristic can be divided into two regions, one for the smaller values of L from where the mechanical tuning characteristic deviates, and the other for the larger values of L, where it follows the half-wavelength behavior. In the former region, the loaded Q of the cavity is low, and the interaction between its different tuning elements is strong. As a result, the varactor tuning voltage has to be restricted within certain limits to avoid spurious operation, frequency switching (distinct from mode switching), noisy output, etc. The latter region is the well-known short-circuit controlled region in which the oscillator is well behaved. There are no limits on the tuning voltage other than those set by the varactor diode itself. In this region, as L is increased, the loaded Q increases, resulting in a decreasing electronic tuning range, which even becomes negative [Fig. 6(b)].

Discussion of Results

It has been observed that the introduction of an electronic tuning arrangement causes only minor changes in the tuning characteristic of a mechanically tuned oscillator which follows the half-wavelength behavior. The general nature of the variation of the electronic tuning range with mechanical tuning has also been established.

It might be suggested that these observations refer only to the particular configurations used and not to the general family of electromechanically tuned Gunn oscillators in distributed circuits. But it

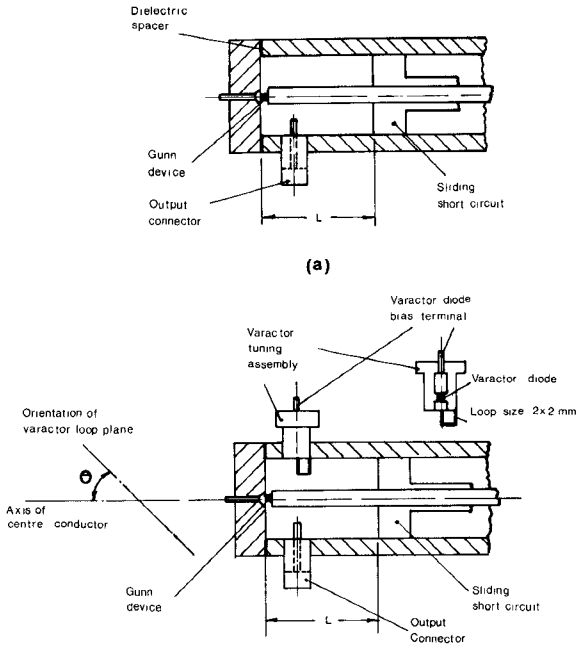

Fig. 4. Coaxial cavity configuration for (a) mechanically tuned and (b) electromechanically tuned Gunn oscillator.

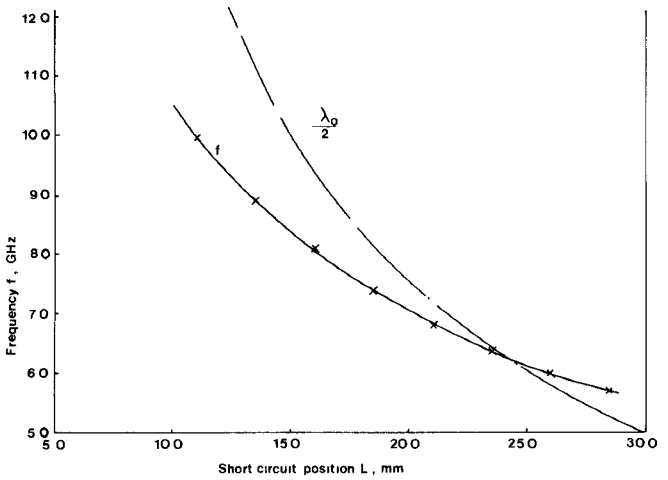

Fig. 5. Mechanical tuning characteristic of the configuration shown in Fig. 4(a). Gunn device CXY 19/35 $V_G = 12{,}6$ V.

should be remembered that these observations are based on the limitations imposed by one of the (perfect) reflecting planes of the cavity. Thus their generality can be justified on the basis that a perfect reflecting plane has a unity reflection coefficient for all frequencies, a magnitude which cannot be obtained, for all frequencies, by any other element or combination of elements other than a perfect reflecting plane itself.

Summary and Conclusions

The general nature of the tuning characteristics of electromechanically tuned Gunn oscillators has been established. It has been shown that the electronic (varactor) tuning range is correlated to the mechanical tuning characteristics; the exact nature of this correlation largely depends upon the propagating characteristics of the system in which the cavity is formed.

Since the observations are independent of the semiconductor microwave source used, it is suggested that these limitations are imposed by a distributed circuit on a point source.

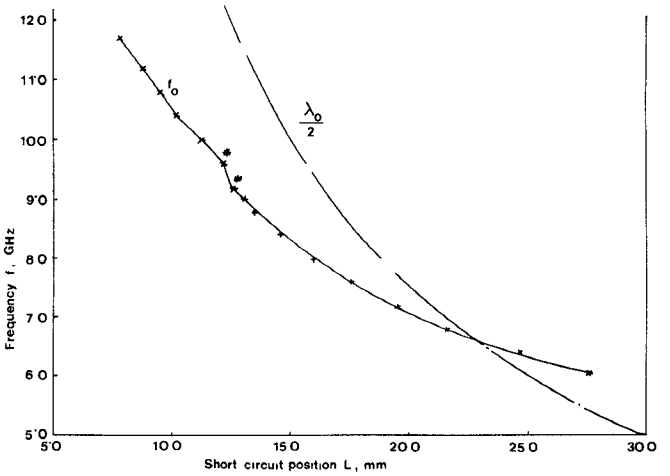

(a)

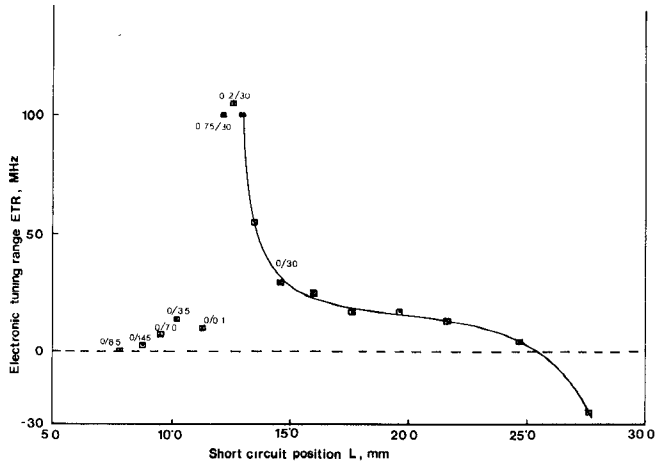

(b)

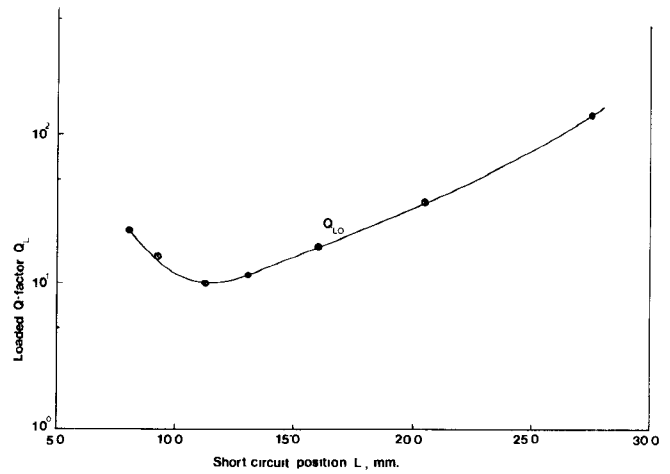

(c)

Fig. 6. (a) Mechanical tuning characteristic of the configuration shown in Fig. 4(b). Asterisks indicate noisy output at zero varactor bias. Gunn device CXY 19/35 $V_G = 10{,}0$ V. (b) Electronic tuning characteristic of the configuration shown in Fig. 4(b). Varactor tuning voltage 0–30 V. Figures indicate the limits on varactor tuning voltage for stable operation. (c) Loaded Q factor (at zero varactor bias, Q_{L0}) versus short-circuit position for the configuration of Fig. 4(b).

It is hoped that this contribution will help designers of electromechanically tuned solid-state ("point") sources in deciding qualitatively those things which are within the realms of possibility.

References

[1] H. Pollmann, R. W. H. Engelman, W. Frey, and B. G. Bosch, "Load dependence of Gunn-oscillator performance," *IEEE Trans. Microwave Theory Tech. (Special Issue on Microwave Circuit Aspects of Avalanche-Diode and Transferred Electron Devices)*, vol. MTT-18, pp. 817–827, Nov. 1970.

[2] B. C. Taylor, S. J. Fray, and S. E. Gibbs, "Frequency-saturation effects in transferred electron oscillators," *IEEE Trans. Microwave Theory Tech. (Special Issue on Microwave Circuit Aspects of Avalanche-Diode and Transferred Electron Devices)*, vol. MTT-18, pp. 799–807, Nov. 1970.

[3] W. C. Tsai, F. J. Rosenbaum, and L. A. MacKenzie, "Circuit analysis of waveguide-cavity Gunn-effect oscillator," *IEEE Trans. Microwave Theory Tech. (Special Issue on Microwave Circuit Aspects of Avalanche-Diode and Transferred Electron Devices)*, vol. MTT-18, pp. 808–817, Nov. 1970.

[4] C. P. Jethwa and R. L. Gunshor, "An analytical equivalent circuit representation of waveguide-mounted Gunn oscillators," *IEEE Trans. Microwave Theory Tech.*, vol. MTT-20, pp. 565–572, Sept. 1972.

[5] R. L. Eisenhart and P. J. Khan, "Some tuning characteristics and oscillation conditions of a waveguide-mounted transferred-electron diode oscillator," *IEEE Trans. Electron Devices*, vol. ED-19, pp. 1050–1055, Sept. 1972.

[6] R. B. Smith and P. W. Crane, "Varactor-tuned Gunn-effect oscillator," *Electron. Lett.*, vol. 6, pp. 139–140, 1970.

[7] B. J. Downing and F. A. Myers, "Broadband (1.95-GHz) varactor-tuned *X*-band Gunn oscillator," *Electron. Lett.*, vol. 7, pp. 407–409, 1971.

[8] J. S. Joshi, "Wide-band varactor-tuned *X*-band Gunn oscillators in full-height waveguide cavity," *IEEE Trans. Microwave Theory Tech.* (Short Papers), vol. MTT-21, pp. 137–139, Mar. 1973.

[9] J. Bravman and J. Frey, "High performance varactor tuned Gunn oscillators," in *Proc. 3rd Cornell Elec. Eng. Conf. High Frequency Generation and Amplification: Devices and Applications*, Cornell Univ., Ithaca, N.Y., pp. 335–339.

[10] J. S. Joshi, "Post-coupled waveguide-cavity Gunn oscillators with varactor tuning," Mullard (Hazel Grove) Ltd., Rep. JJ 190472, Apr. 1972.

[11] ——, "Performance characteristics of mechanically tunable coaxial cavity Gunn oscillators with varactor tuning," Mullard (Hazel Grove) Ltd., Rep. JJ 301172, Nov. 1972.

Two Oversize Waveguide-Polarization Diplexers

J. T. MENDONÇA

***Abstract*—Two new types of quasi-optical waveguide-polarization diplexers are described. They are based on the use of a metal grating, or a dielectric plate at Brewster's angle, placed in an oversize circular 3-port junction. Their performances are measured at a wavelength of 4.28 mm in a standard microwave circuit and at 337 μm with the HCN laser beam.**

At millimeter and submillimeter wavelengths, quasi-optical circuit techniques were found to be more effective than more standard waveguide approaches. Here we report experimental results obtained with two types of quasi-optical polarization diplexers which once more confirm the preceding assertion.

These two systems use metal grids of parallel wires and dielectric plates at Brewster's incidence, and we shall call them for simplicity grid diplexer and plate diplexer.

A cross section of the grid diplexer is shown in Fig. 1. It consists of a circular 3-port junction, in the middle of which is placed a grid of parallel metal strips at 45° of incidence. An appropriate mechanical system permits the orientation of the strips in the right position with an accuracy of 0.1°. The circular waveguides of the junction have a diameter of 28.3 mm which is a standard dimension for the *X* band.

Two transition cones connect the output arms of the junction to the single-mode waveguide size of the working band (for instance, the 4-mm band). Each of the transition cones is continued by a circular-to-rectangular transition in the single-mode waveguide size, which is connected to a conventional rectangular waveguide. The position of this rectangular waveguide must agree with the electric polarization wanted in each of the outputs.

The input arm is connected with the free-space radiation by a circular horn. In a completely guided application this horn must be replaced by a third conical transition.

The grid we have used is of parallel aluminum strips with a width of 5 μm and period of 10 μm, made by photolithographic techniques on a polyethylene substrate approximately 1 mm thick, as described by Auton [1].

Manuscript received January 21, 1973; revised May 14, 1973.

The author is with the Association Euratom–CEA sur la Fusion, Département de Physique du Plasma et de la Fusion Contrôlée, Centre d'Études Nucléaires, Boîte Postale n° 6, 92260 Fontenay-Aux-Roses, France.

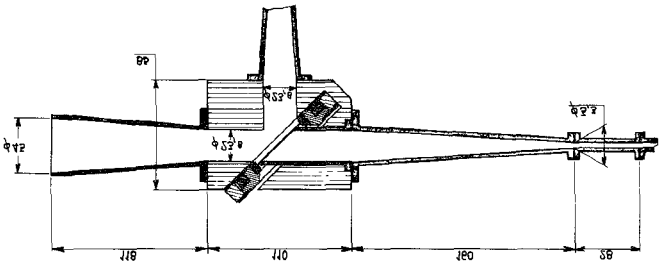

Fig. 1. Cross section of the grid diplexer. (Dimensions are in millimeters.)

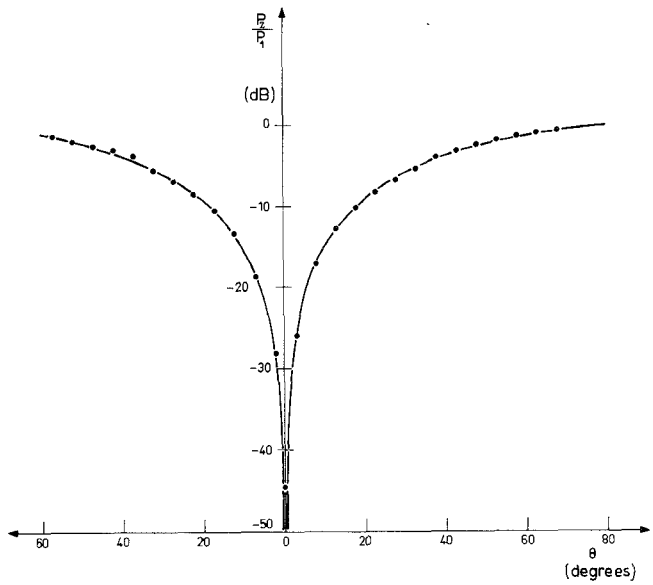

Fig. 2. Normalized power at the transmission output of the grid diplexer P_2/P_1 versus angle of polarization θ, for 70 GHz.

Let us suppose that the strips are parallel to the plane of incidence and that the incident field is also polarized parallel to this plane. By the well-known properties of the metallic grids [2] almost all of the incident power P_1 must be reflected and leave the junction by the reflection arm, and the power P_2 at the transmission arm must be zero. In practice this zero will be due not only to the filtering properties of the grid but also to the filtering properties of the rectangular waveguide at the output, because by its position it transmits only the electric field polarized perpendicularly to the plane of incidence.

Now, if the plane of polarization of the incident field makes an angle θ with the plane of incidence, an ideal diplexer must give the normalized power $P_2/P_1 = \sin^{-2}\theta$ at the transmission output.

Values of P_2/P_1, in decibel, versus the angle of polarization θ have been measured at 70 GHz and are shown in Fig. 2. They are in agreement with the theoretical values.

The experimental minimum $(P_2/P_1)_0 = -45$ dB, which we can name the directivity of the diplexer, is particularly important because the little variations of angle $\delta\theta$ that can be read by the diplexer are of the order of arctan $(P_2/P_1)_0^{1/2}$. In a conventional fin-line diplexer for the 4-mm and the 2-mm band the directivity is about 30 dB, which means that the quasi-optical diplexer described here is much more accurate.

Measurements of directivity of the grid diplexer have also been made at 890 GHz with the HCN laser beam. In this case neither the cone transitions nor the waveguides shown in Fig. 1 are necessary, and the 3-port junction alone is used. The result is $(P_2/P_1)_0 = -31$ dB.

It must be pointed out that the dielectric substrate of the grid introduces some asymmetry in the diplexer. If it was symmetric the normalized power P_3/P_1 at the reflection arm, for $\theta = 90°$, would be of the same order of the above mentioned directivity, say −45 dB. But the dielectric substrate has a nonnegligible reflectivity. A theoretical calculation based on the equivalence with the theory of the trans-